Preprints (www.preprints.org) | NOT PEER-REVIEWED | Posted: 6 October 2021 doi:10.20944/preprints202103.0611.v2

TPEN Selectively Eliminates Lymphoblastic B cells from Bone Marrow Pediatric Acute Lymphoblastic Leukemia Patients

Mendivil-Perez M[1], Velez-Pardo C[1], Quiroz-Duque LM[2], Restrepo-Rincon A[2], Valencia-Zuluaga NA[2], Marlene Jimenez-Del-Rio M[1,*]

1 Neuroscience Research Group, Medical Research Institute, Faculty of Medicine, University of Antioquia (UdeA), Calle 70 No. 52–21, and Calle 62 # 52–59, Building 1, Room 412; SIU Medellin, Colombia; MM-P: miguelangelmendivil@gmail.com; CV-P: calberto.velez@udea.edu.co; MJ-del-Rio: marlene.jimenez@udea.edu.co

2 Hospital Pablo Tobon Uribe, Pediatric Oncology Unit, Calle 78b #69–240, Medellin, Colombia; LMQ-D: lquiroz@hptu.org.co; AR-R: alresrin@hotmail.com; NAV-Z: natyval82@hotmail.com

* Correspondence: MJ-del-Rio: marlene.jimenez@udea.edu.co

© 2021 by the author(s). Distributed under a Creative Commons CC BY license.

Preprints (www.preprints.org) | NOT PEER-REVIEWED | Posted: 6 October 2021 doi:10.20944/preprints202103.0611.v2

Abstract: B-cell acute lymphoblastic leukemia (B-ALL) is a hematologic disorder characterized by the abnormal proliferation and accumulation of immature B-lymphoblasts arrested at various stages of differentiation. Despite advances in treatment, a significant percentage of pediatric patients with precursor B-ALL still relapse. Therefore, alternative therapies are needed to improve the cure rates for pediatric patients. TPEN (N, N, N', N'-tetrakis(2-pyridylmethyl)-ethylenediamine).is a pro-oxidant agent capable of selectively inducing apoptosis in leukemia cells. Consequently, it has been suggested that TPEN could be a potential agent for oxidative therapy. However, it is not yet known whether TPEN can selectively destroy leukemia cells in a more disease-like model, for example, the bloodstream and bone marrow (BM), in vitro. This investigation is an extension of a previous study that dealt with the effect of TPEN on ex vivo isolated/purified refractory B-ALL cells. Here, we evaluated the effect of TPEN on whole BM from nonleukemic patients (control) or pediatric patients diagnosed with de novo B-ALL or refractory B-ALL cells by analyzing the hematopoietic cell lineage marker CD34/CD19. Although TPEN was innocuous to nonleukemic BM (n=3), we found that TPEN significantly induced apoptosis in de novo (n = 5) and refractory B-ALL (n = 6) leukemic cell populations. Moreover, TPEN significantly increased the counts of cells positive for the oxidation of the stress sensor protein DJ-1, a sign of the formation of H2O2, and significantly increased the counts of cells positive for the pro-apoptotic proteins TP53, PUMA, and CASPASE-3 (CASP-3), indicative of apoptosis, in B-ALL cells. We demonstrate that TPEN selectively eliminates B-ALL cells independent of age, diagnosis status (de novo or refractory), sex, karyotype, or immunophenotype. Understanding TPEN-induced cell death in leukemia cells provides insight into more effective therapeutic oxidation-inducing anticancer agents.

Preprints (www.preprints.org) | NOT PEER-REVIEWED | Posted: 6 October 2021 doi:10.20944/preprints202103.0611.v2

Keywords: acute leukemia; caspase-3; chemoresistant; DJ-1; TP53; PUMA; reactive oxygen species; signaling; TPEN

Preprints (www.preprints.org) | NOT PEER-REVIEWED | Posted: 6 October 2021 doi:10.20944/preprints202103.0611.v2

Introduction

B-cell acute lymphoblastic leukemia (B-ALL) is a neoplasm of immature B-cell pre-cursors characterized by the abnormal proliferation and accumulation of immature lymphoblasts arrested at the pre- to pro-B cell or pro-B cell stages [1]. B-ALL typically affects children younger than 6 years but can also affect older children and adult populations [2, 3]. The diagnosis is established by immunophenotyping, commonly by flow cytometry, which shows an immature B lineage. Many cases of B-ALL harbor recurrent chromosomal abnormalities, which are critical determinants of prognosis [4]. Despite intensive classical chemotherapy and other available targeted therapies [5], approximately 20% of children with precursor B-ALL relapse (e.g., [6]). Therefore, alternative therapies are needed to im-prove cure rates for pediatric patients with B-cell relapsed leukemia.

Oxidation therapy offers an important therapeutic opportunity to eliminate B-ALL [7-9]. The administration of exogenous agents aimed at the selective production of reactive oxygen species (ROS) can impair the redox balance of leukemia cells [10, 11] leading to apoptosis, a regulated cell death process [12], which is commonly altered in those cells [13-15]. Accordingly, several ROS-producing agents have selectively enhanced cancer ROS levels and apoptosis [16, 17], including the lipid-soluble zinc metal chelator TPEN (N, N, N', N'-tetrakis(2-pyridylmethyl)-ethylenediamine). Remarkably, TPEN induces apoptosis in several cancer cell lines [18-23], including leukemia cells [24] through the generation of high ROS levels and oxidative stress (OS) [25-27]. Mechanistically, it has been shown to induce apoptosis through two independent but complementary pathways triggered by hydrogen peroxide (H_2O_2). In fact, TPEN/(H_2O_2) activates the transcription factors NF-κB, TP53, and c-JUN; upregulates proapoptotic proteins such as BAX and PUMA; induces the loss of

Preprints (www.preprints.org) | NOT PEER-REVIEWED | Posted: 6 October 2021 doi:10.20944/preprints202103.0611.v2

mitochondrial membrane potential (ΔΨm), and activates the protease CASP-3 and NADH-dependent oxidoreductase AIF, all of which lead to nuclear chroma-tin condensation and DNA fragmentation, typical of apoptosis [25-27]. Although the cytotoxic effect of TPEN on leukemia cells has been tested either in model cells (e.g., ALL Jurkat cells [25], chronic myeloid leukemia K562 cells [26], and acute promyelocytic NB4 cells [24]), or in ex vivo and isolated/purified cells from leukemia bone marrow samples [27], no data are available to establish whether TPEN induces apoptosis in B-cells from ex vivo whole bone marrow (BM) pediatric patients diagnosed with de novo B-ALL.

This investigation is an extension of a previous study that dealt with the effect of TPEN on *ex vivo* isolated refractory B-ALL cells [27]. Here we evaluated the effect of TPEN on whole BM from nonleukemic patients (n=3) or pediatric patients diagnosed with de novo B-ALL (n=5) and refractory (n=6) B-ALL cells by analyzing the hematopoietic cell lineage markers CD34/CD19. We found that TPEN induces apoptosis in B-ALL cells through activation of TP53, PUMA, and CASP-3. Taken together, these observations suggest that TPEN efficiently eliminates B-ALL cells in pediatric patients with de novo and refractory B-ALL.

Preprints (www.preprints.org) | NOT PEER-REVIEWED | Posted: 6 October 2021 doi:10.20944/preprints202103.0611.v2

Materials and Methods

Experiments with Bone Marrow Samples from Chemoresistant Leukemia Pediatric Patients

Bone marrow (BM) samples were collected from 3 nonleukemic patients and 11 pediatric patients diagnosed with de novo B-ALL (n = 5) or refractory B-ALL (n = 6) admitted to the Pediatric Oncology Unit of the Pablo Tobon Uribe Hospital (HPTU), Medellin, Colombia. Written informed consent was obtained in accordance with the Ethics Committee for Research Act no. 17-10-697 (17 May 2017) and the HPTU 08/2018, and with the 1964 Helsinki declaration and its later amendments or comparable ethical standards. The BM samples (100 µL) were directly plated in 96-well plates and incubated without or with TPEN (50–500 µM) for 24 h at 37 °C in a humidified atmosphere with 5% CO_2. TPEN was diluted to a 0.01 M (10 mM) stock solution in 5% ethanol (ethyl alcohol Merck, Darmstadt, Germany) in PBS. Before use in vitro, the stock solution was further diluted to 0.001 mM (1 mM) in 0.5% ethanol. The final concentration of ethanol in the culture well was 0.25%-0.025%.

Simultaneous Analysis of CD34, CD19, and caspase-3 or PUMA by Flow Cytometry in Bone Marrow (BM) cells from Chemoresistant Leukemia Pediatric Patients

Flow cytometry acquisition was used to determine the percentage of CD34/CD19/CASPASE−3 (CASP-3) triple-positive cells. After each treatment with or without TPEN, erythrocytes were lysed, and BM cells were washed with PBS and permeabilized with 0.2% Triton X-100 plus 1.5% bovine serum albumin (BSA) for 30 min and simultaneously incubated for 20 min at 37 °C in the dark with mouse anti-human CD34-PE and CD19-PEcy7 antibodies (1:200, BD Biosciences, San Jose, USA) and CASP-3

Preprints (www.preprints.org) | NOT PEER-REVIEWED | Posted: 6 October 2021 doi:10.20944/preprints202103.0611.v2

(rabbit, Millipore, cat. #AB3623, St. Louis, USA) or PUMA (rabbit, Abcam, cat ab-9643, Burlingame, USA). Subsequently, the cells were washed and incubated with (1:500) DyLight donkey anti-rabbit (488 nm, cat # DI-2488). Then, the cells were analyzed using a BD LSRFortessa II flow cytometer (BD Biosciences, San Jose, USA), and 20,000 events were acquired for analysis. Quantitative data and figures were obtained using FlowJo 7.6.2 Data Analysis Software.

Detection of Oxidized (Cys106) DJ-1/CASP-3 and PUMA/TP53 by Flow Cytometry in Bone Marrow (BM) Cells from Chemoresistant Leukemia Pediatric Patients

After each treatment with or without TPEN, RBCs were lysed in 10 mL of standard RBC lysis solution (Qiagen, cat #158902). The mixture was centrifuged for 10 min at 2000 RPM. Then, the purified BM cells were washed with PBS and permeabilized with 0.2% Triton X-100 plus 1.5% bovine serum albumin (BSA) for 30 min; the cells were washed and incubated with anti-p53 (mouse, Millipore, cat MA5-12453), PUMA (rabbit, Abcam, cat no. ab-9643), CASP-3 (rabbit, Millipore, cat no. AB3623) and oxidized DJ-1 (spanning residue C106 of Human PARK7/DJ1; oxidized to produce cysteine sulfonic (SO_3) acid; mouse, Millipore, cat # MABN1773). Primary antibodies (1:500) were diluted in PBS containing 0.1% BSA. Subsequently, the cells were washed and incubated with (1:500) DyLight donkey anti-rabbit (594 nm, cat no. DI-1094) or -mouse (488 nm, cat no. DI-2488) secondary antibodies for 30 min. at RT in the dark. After washing with PBS, the cells were suspended in 500 µL of PBS. The analysis was performed on a BD LSRFortessa II flow cytometer (BD Biosciences, San Jose, USA). Cells without primary antibodies served as a negative control. For the assessment, we acquired 20,000 events and quantitative data and figures were obtained using FlowJo 7.6.2 Data Analysis Software.

Preprints (www.preprints.org) | NOT PEER-REVIEWED | Posted: 6 October 2021 doi:10.20944/preprints202103.0611.v2

Statistical Analysis

Statistical analyses were performed using GraphPad Prism 6 scientific software (GraphPad, Software, Inc. La Jolla, CA, USA). One-way ANOVA with Tukey's post hoc test was used to compare the differences between the multiple experimental groups (i.e., nonleukemic and leukemic samples) or Student's t-test was used to compare the differences in a particular group (i.e., nonleukemic or leukemic samples). A p-value <0.05 (*), <0.01 (**) and <0.001 (***) was considered statistically significant.

Preprints (www.preprints.org) | NOT PEER-REVIEWED | Posted: 6 October 2021 doi:10.20944/preprints202103.0611.v2

Results

Profiles from nonleukemic and pediatric B-ALL Patients

Table 1 shows the characteristic profiles of 3 nonleukemic patients and 11 pediatric patients diagnosed with de novo B-ALL (n = 5) and refractory B-ALL (n = 6). The disease was conventionally diagnosed by a complete white blood cell count (WBC), a blast cell count (represented as the percentage of blast cells in the blood), and bone marrow immunophenotypic tests in four male and seven female children–adolescents aged between 2.5 and 16 years. There were no significant differences in the age of diagnosis between the de novo B-ALL and refractory B-ALL patients. As expected, karyotype analysis revealed a complex karyotype (i.e., the presence of more than or equal to five chromosomal abnormalities, e.g., codes 72750 and 48983) or recurrent aberrations (e.g., codes 04168 and 81571). Immuno-phenotypic analysis showed 61%–97% B-cells with a high degree of immunophenotypic heterogeneity of the malignant cell population. All the cells expressed CD19+, a typical B-cell lineage marker, and CD34+, a hematopoietic stem cell marker. The phenotypic markers CD34 and CD19 were selected for further analysis.

TPEN Induces a Reduction in the CD34+/CD19+ Cell Population, and Activation of CASP-3 in Lymphoblastic B-Cells Derived from Chemoresistant Bone Marrow Leukemia Pediatric Patients

First, we evaluated whether TPEN induced apoptosis in three bone marrow samples (BMs) diagnosed with de novo B-ALL (code #72750, #19105, and #62232, Table 1). The BM samples were left untreated or exposed to TPEN (50, 100, 200, and 500 μM) for 24 h. Flow cytometry analysis (Figure 1A) showed that TPEN significantly reduced the CD34+/CD19+

Preprints (www.preprints.org) | NOT PEER-REVIEWED | Posted: 6 October 2021 doi:10.20944/preprints202103.0611.v2

cell population in a concentration-independent manner, for example, 93 ± 3.4% (untreated) vs. 86.3 ± 10.7% (50), 71 ± 7.2% (100), 66.3 ± 5.7% (200), and 62.3 ± 8% (500 μM TPEN). Further analysis (red broken lines in Figure 1B) showed that TPEN at 50, 100, 200, and 500 (μM) induced the activation of CASP-3 by ~57%, ~86%, ~86%, and ~88%, respectively. Because TPEN (100 μM) was the minimal concentration at which CASP-3 was activated as an indicative marker of apoptosis (Figure 1C, i.e., ~sevenfold increase CASP-3 activation in CD34+/CD19+ B-cells, n = 3), this concentration was selected for further experimental procedures.

To validate the effect of TPEN on B-cells, we performed a flow cytometry double analysis of the CD19+/ CD34+ population in nonleukemic cells (n=3) and de novo (n = 5) and refractory (n = 6) B-ALL cells. Except in nonleukemic cells, TPEN reduced the B-ALL blast population (Figure 2A). While the mean blast percentage in untreated cells was 62.6 ± 20.5%, TPEN (100 μM) significantly reduced the blast population to 42.6 ± 20.5% (i.e., ~32% reduction, Figure 2B).

Likewise, flow cytometry three-dimensional (3D) density plot analysis (CD19+/CD34+/CASP-3+) indicated that TPEN increased the activation of CASP-3 (~632%) in leukemic B cells (e.g., 31.5 ± 13.2%) compared with untreated cells (4.30 ± 1%, Figure 3A, and 3B), but no effect on CASP-3 expression was observed in nonleukemic cells. Since there were no statistically significant differences between samples diagnosed with de novo (n = 5) and refractory (n = 6) B-ALL untreated or treated with TPEN (Table 1), we pooled de novo and refractory data (hereafter code number in black) for further statistical analysis.

Preprints (www.preprints.org) | NOT PEER-REVIEWED | Posted: 6 October 2021 doi:10.20944/preprints202103.0611.v2

TPEN Simultaneously, Induces Oxidation of DJ-1 and Activation of CASP-3 in Cells Derived from BM Chemoresistant Leukemia Patients

Next, we investigated whether TPEN induces the oxidation of the stress sensor protein DJ-1 and activates CASP-3 in BM cells. As shown in Figure 4A, TPEN increased the double staining of oxidized DJ-1+/CASP-3+ in the B-ALL cell population (e.g., 16.25 ± 11%) compared with untreated cells (1.1 ± 0.8%, Figure 4B) by 94%. TPEN had no significant effect on DJ-1+/CASP-3+ expression in nonleukemic cells.

TPEN Upregulates PUMA Protein in Cells Derived from Chemoresistant Leukemia Patients

The above observations prompted us to evaluate whether TPEN induces the activation of the protein PUMA, a death marker, in control or B-ALL cells. Flow cytometry 3D density plot analysis (CD34+/CD19+/PUMA+) indicated that TPEN upregulated PUMA protein in leukemic B cells (27.5 ± 9.1%) compared with untreated BM cells (e.g., 5.25 ± 2.7%, Figure 5A, B) by 81%. There was no effect of TPEN on nonleukemic cells.

TPEN Simultaneously, Upregulates PUMA Protein and TP53 Transcription Factors in Cells Derived from Chemoresistant Leukemia Patients

Then, we evaluated whether TPEN induces

the activation of the transcription factor TP53 concurrently with the proapoptotic protein PUMA in BM samples from B-leukemia patients. As shown in Figure 6A, TPEN

Preprints (www.preprints.org) | NOT PEER-REVIEWED | Posted: 6 October 2021 doi:10.20944/preprints202103.0611.v2

significantly increased double PUMA+/TP53+ cells (e.g., 3.5 ± 5.4% (untreated) vs. 22 ± 9.5% (treated), Figure 6B) by 67%, but PUMA+/TP53+ cells were almost undetectable in nonleukemic cells.

Preprints (www.preprints.org) | NOT PEER-REVIEWED | Posted: 6 October 2021 doi:10.20944/preprints202103.0611.v2

Discussion

Previous studies have shown that TPEN acts as a pro-oxidant agent capable of inducing selective proapoptotic leukemia cell death through an oxidative stress mechanism, in-volving the generation of H_2O_2, oxidation of stress sensor protein DJ-1, activation of transcription factor TP53 and proapoptotic effector BH3-only protein PUMA, mitochondrial damage, activation of proapoptotic executor protein CASP-3, and disassembly of the nuclei in leukemia cell model (e.g., [25, 26]) and in *ex vivo* isolated refractory leukemia cells from ALL bone marrow samples [27]. Consequently, it has been suggested that TPEN could be a potential agent for oxidative therapy. However, it is not yet known whether TPEN can selectively destroy leukemia cells in a more disease-like model, for example, the bloodstream and bone marrow (BM). The BM is an important microenvironment in which deranged lymphocyte proliferation (e.g., B-ALL) occurs [28]. Since BM is routinely examined for diagnosis and disease prognosis, it represents an important source of biological material and clinical information. Here, we report that TPEN specifically induces apoptosis de novo (n = 5, i.e., patients with no clinical history of prior B-ALL disorder or exposed to potentially leukemogenic therapies or agents) and refractory leukemia cells (n = 6) from ex vivo whole bone marrow (n = 11) based on the detection of selected OS signals and cell death markers in CD34+/CD19+ (B-ALL) cells. We found that TPEN significantly in-creased the oxidation of the stress sensor protein DJ-1 as a marker of OS and increased the positive cell signal for the proapoptotic proteins TP53, PUMA, and CASPASE-3, as indicated by apoptotic cell death. Therefore, in agreement with previous work [25, 27], TPEN provokes apoptosis in lymphoblastic cells, for example, in T-ALL and B-ALL cells, through activation of the intrinsic apoptotic pathway [12]. This investigation, however, differs from the previous

Preprints (www.preprints.org) | NOT PEER-REVIEWED | Posted: 6 October 2021 doi:10.20944/preprints202103.0611.v2

investigation. First, TPEN induces apoptosis in *ex vivo* whole BM B-ALL cells in a dose-independent manner. Indeed, while the toxic dose of TPEN on ex vivo B-ALL cells from BM is between 100 μM and 500 μM (this work), the toxic concentration of TPEN in in vitro model leukemia cells and ex vivo isolated/purified T-ALL/B-ALL cells from BM is 5 μM [25, 27]. Therefore, the TPEN concentration should in-crease 20- to 100-fold to be effective in *ex vivo* BM (this work). Clearly, the toxicity of TPEN on cells is lessened by the BM milieu. Taken together, these results suggest that in addition to the toxic concentration, TPEN induces cell death in B-ALL cells independently of experimental conditions (e.g., isolated versus non-isolated cell conditions). This observation is critical for further clinical trials. Interestingly, TPEN has been reported to be harmless to mice (e.g., at 5 mg/kg daily for 4 months [29] or at 10 or 15 mg/kg body weight for seven successive days [30]). Unfortunately, similar pharmacokinetic and pharmacodynamic studies of TPEN in humans are still lacking. Therefore, further studies are needed to establish whether TPEN can be therapeutically applied to patients with leukemia.

How does TPEN provoke apoptosis in B-ALL? Mounting evidence suggests that TPEN induces cell death by generating of H_2O_2 and by acting as a class 5 mitocan [31] or by forming a TPEN-copper complex [19]. In both instances, TPEN chelates active metals such as iron and copper from mitochondrial complexes I–III to convert oxygen (O_2) into anionic superoxide radicals ($O_2^{\cdot-}$), which in turn dismutase into H_2O_2. Since TPEN is also a strong zinc chelator (e.g., [32]), it can directly activate CASP-3 [33]) or can interact with various zinc-containing molecules, including DNA- and RNA-binding proteins (e.g., [34]), and hence can be affected by zinc binding and depletion of cellular proliferation, leading to apoptosis (e.g., [24]). Regardless of the mechanism, we found a significantly increased level

Preprints (www.preprints.org) | NOT PEER-REVIEWED | Posted: 6 October 2021 doi:10.20944/preprints202103.0611.v2

of oxidized OS sensor protein DJ-1 (Cys106-SO3 (sulfonate)), a specific and selective probe indicative of the oxidation of DJ-1 protein by H_2O_2 [35]. In addition, H_2O_2 can indirectly trigger the activation of the transcription factor TP53 through MAPK kinases [36]. Consequently, TP53 activates PUMA [37, 38]. Effectively, we observed a significant in-crease in both TP53 and PUMA proteins according to flow cytometry. Taken together, these observations suggest that TPEN induces apoptosis via activation of TP53 and PUMA. Outstandingly, PUMA represents one of the most potent initiator proapoptotic BH3-only proteins [39]. Indeed, PUMA cooperates with direct activator proteins to pro-mote mitochondrial outer membrane permeabilization [40] and activation of caspases, for example, CASP-3, which plays a central role in the execution phase of cell apoptosis [41]. In this regard, we consistently detected an association of increased CD34/CD19/CASP-3 positive cells with CD34/CD19/DJ-1Cys106-SO_3 positive cells. These data suggest that CD34+/CD19+ cells stressed by TPEN ended up in the dismantling of nuclei by CASP-3. Interestingly, CASP-3+ and PUMA+ cells showed a similar percentage of activation as CD34+/CD19+ cells. Taken together, these observations imply that TPEN induces apoptosis in a cascade-like mechanism as follows: TPEN >>> TP53 > PUMA >> CASP-3 > cell death.

Conclusion

We have demonstrated that TPEN triggers apoptosis in ex vivo whole bone marrow cells diagnosed with de novo B-ALL and refractory B-ALL in pediatric patients independently of age, diagnosis status, sex, karyotype, or immunophenotype through a similar mechanism as described previously in a Jurkat cell model of ALL [25] as well as ex vivo BM-isolated/purified ALL cells [27]. Although leukemic cell samples are still limited, our present data support the view that TPEN effectively kills B-ALL cells. Therefore, TPEN is a potential

Preprints (www.preprints.org) | NOT PEER-REVIEWED | Posted: 6 October 2021 doi:10.20944/preprints202103.0611.v2

agent to be tested in the clinic. However, further investigation is needed to confirm or dismiss this assumption.

Preprints (www.preprints.org) | NOT PEER-REVIEWED | Posted: 6 October 2021 doi:10.20944/preprints202103.0611.v2

Institutional Review Board Statement: All procedures performed in studies involving human participants were in accordance with the ethical standards of the Ethics Committee for Research Act no. 17-10-697 and HPTU 08/2018 from HPTU, and with the 1964 Helsinki declaration and its later amendments or comparable ethical standards.

Funding Statement. This study was funded by "Fundación Alfonso Moreno Jaramillo" grant #2018–20454 to CV-P. The funders had no role in study design, data collection, and analysis, decision to publish, or preparation of the manuscript.

Conflict of interest. The authors have declared that no competing interests exist.

Informed Consent Statement: Informed consent was obtained from pediatric ex vivo B-ALL collected in the study.

Data Availability Statement. The data used to support the findings of this study are available from the corresponding author upon request.

Sample Availability: Not available.

Author Contributions

Author Contributions: Conceptualization, C.V.-P. and M.J.-del-R.; methodology, M.M.-P.; validation, C.V.-P. and M.M.-P.; formal analysis, C.V.-P., M.M.-P., and M.J.-del-R.; investigation, C.V.-P., M.M.-P., L.M.Q.-D., A.R.-R., N.A.V.-Z., and M.J.-del-R.; data curation, M.M.-P. and M.J.-del-R.; writing—original draft preparation, C.V.-P. and M.J.-del-R.; writing—review and editing, C.V.-P., M.M.-P., and M.J.-del-R.; supervision, C.V.-P., M.M.-P., L.M.Q.-D, A.R.-R., N.A.V.-Z., and M.J.-del-R.; project administration, M.J.-del-R.; funding acquisition, C.V.-P., whole bone marrow samples and clinical data acquisition

Preprints (www.preprints.org) | NOT PEER-REVIEWED | Posted: 6 October 2021 doi:10.20944/preprints202103.0611.v2

from de novo and refractory B-ALL patients, L.M.Q.-D, A.R.-R., and N.A.V.-Z. All authors have read and agreed to the published version of the manuscript.

Preprints (www.preprints.org) | NOT PEER-REVIEWED | Posted: 6 October 2021 doi:10.20944/preprints202103.0611.v2

References

1. Ramyar, A., et al., *Cytologic phenotypes of B-cell acute lymphoblastic leukemia-a single center study.* Iran J Allergy Asthma Immunol, 2009. **8**(2): p. 99-106.
2. Hunger, S.P. and C.G. Mullighan, *Acute Lymphoblastic Leukemia in Children.* N Engl J Med, 2015. **373**(16): p. 1541-52.
3. O'Dwyer, K.M. and J.L. Liesveld, *Philadelphia chromosome negative B-cell acute lymphoblastic leukemia in older adults: Current treatment and novel therapies.* Best Pract Res Clin Haematol, 2017. **30**(3): p. 184-192.
4. Woo, J.S., M.O. Alberti, and C.A. Tirado, *Childhood B-acute lymphoblastic leukemia: a genetic update.* Exp Hematol Oncol, 2014. **3**: p. 16.
5. Rafei, H., H.M. Kantarjian, and E.J. Jabbour, *Recent advances in the treatment of acute lymphoblastic leukemia.* Leuk Lymphoma, 2019. **60**(11): p. 2606-2621.
6. Oskarsson, T., et al., *Relapsed childhood acute lymphoblastic leukemia in the Nordic countries: prognostic factors, treatment and outcome.* Haematologica, 2016. **101**(1): p. 68-76.
7. Liu, J. and Z. Wang, *Increased Oxidative Stress as a Selective Anticancer Therapy.* Oxid Med Cell Longev, 2015. **2015**: p. 294303.
8. Zou, Z., et al., *Induction of reactive oxygen species: an emerging approach for cancer therapy.* Apoptosis, 2017. **22**(11): p. 1321-1335.
9. Kim, S.J., H.S. Kim, and Y.R. Seo, *Understanding of ROS-Inducing Strategy in Anticancer Therapy.* Oxid Med Cell Longev, 2019. **2019**: p. 5381692.
10. Prieto-Bermejo, R., et al., *Reactive oxygen species in haematopoiesis: leukaemic cells take a walk on the wild side.* J Exp Clin Cancer Res, 2018. **37**(1): p. 125.

Preprints (www.preprints.org) | NOT PEER-REVIEWED | Posted: 6 October 2021 doi:10.20944/preprints202103.0611.v2

11. Perillo, B., et al., *ROS in cancer therapy: the bright side of the moon.* Exp Mol Med, 2020. **52**(2): p. 192-203.

12. Galluzzi, L., et al., *Molecular mechanisms of cell death: recommendations of the Nomenclature Committee on Cell Death 2018.* Cell Death Differ, 2018. **25**(3): p. 486-541.

13. Samudio, I., et al., *Apoptosis in leukemias: regulation and therapeutic targeting.* Cancer Treat Res, 2010. **145**: p. 197-217.

14. Cassier, P.A., et al., *Targeting apoptosis in acute myeloid leukaemia.* Br J Cancer, 2017. **117**(8): p. 1089-1098.

15. Sillar, J.R. and A.K. Enjeti, *Targeting Apoptotic Pathways in Acute Myeloid Leukaemia.* Cancers (Basel), 2019. **11**(11).

16. Galadari, S., et al., *Reactive oxygen species and cancer paradox: To promote or to suppress?* Free Radic Biol Med, 2017. **104**: p. 144-164.

17. Tang, Z.M., et al., *Biodegradable Nanoprodrugs: "Delivering" ROS to Cancer Cells for Molecular Dynamic Therapy.* Adv Mater, 2020. **32**(4): p. e1904011.

18. Hashemi, M., et al., *Cytotoxic effects of intra and extracellular zinc chelation on human breast cancer cells.* Eur J Pharmacol, 2007. **557**(1): p. 9-19.

19. Fatfat, M., et al., *Copper chelation selectively kills colon cancer cells through redox cycling and generation of reactive oxygen species.* BMC Cancer, 2014. **14**: p. 527.

20. Rahal, O.N., et al., *Chk1 and DNA-PK mediate TPEN-induced DNA damage in a ROS dependent manner in human colon cancer cells.* Cancer Biol Ther, 2016. **17**(11): p. 1139-1148.

Preprints (www.preprints.org) | NOT PEER-REVIEWED | Posted: 6 October 2021 doi:10.20944/preprints202103.0611.v2

21. Stuart, C.H., et al., *Prostate-specific membrane antigen-targeted liposomes specifically deliver the Zn(2+) chelator TPEN inducing oxidative stress in prostate cancer cells.* Nanomedicine (Lond), 2016. **11**(10): p. 1207-22.

22. Soto-Mercado, V., et al., *TPEN Exerts Antitumor Efficacy in Murine Mammary Adenocarcinoma Through an H2O2 Signaling Mechanism Dependent on Caspase-3.* Anticancer Agents Med Chem, 2018. **18**(11): p. 1617-1628.

23. Yu, Z., et al., *Zinc chelator TPEN induces pancreatic cancer cell death through causing oxidative stress and inhibiting cell autophagy.* J Cell Physiol, 2019. **234**(11): p. 20648-20661.

24. Zhu, B., et al., *Zinc Depletion by TPEN Induces Apoptosis in Human Acute Promyelocytic NB4 Cells.* Cell Physiol Biochem, 2017. **42**(5): p. 1822-1836.

25. Mendivil-Perez, M., C. Velez-Pardo, and M. Jimenez-Del-Rio, *TPEN induces apoptosis independently of zinc chelator activity in a model of acute lymphoblastic leukemia and ex vivo acute leukemia cells through oxidative stress and mitochondria caspase-3- and AIF-dependent pathways.* Oxid Med Cell Longev, 2012. **2012**: p. 313275.

26. Rojas-Valencia, L., C. Velez-Pardo, and M. Jimenez-Del-Rio, *Metal chelator TPEN selectively induces apoptosis in K562 cells through reactive oxygen species signaling mechanism: implications for chronic myeloid leukemia.* Biometals, 2017. **30**(3): p. 405-421.

27. Mendivil-Perez, M., et al., *TPEN exerts selective anti-leukemic efficacy in ex vivo drug-resistant childhood acute leukemia.* Biometals, 2021. **34**(1): p. 49-66.

28. Duarte, D., E.D. Hawkins, and C. Lo Celso, *The interplay of leukemia cells and the bone marrow microenvironment.* Blood, 2018. **131**(14): p. 1507-1511.

Preprints (www.preprints.org) | NOT PEER-REVIEWED | Posted: 6 October 2021 doi:10.20944/preprints202103.0611.v2

29. Li, B., et al., *Zinc is essential for the transcription function of Nrf2 in human renal tubule cells in vitro and mouse kidney in vivo under the diabetic condition.* J Cell Mol Med, 2014. **18**(5): p. 895-906.

30. Xiao, Z., et al., *Zinc chelation inhibits HIV Vif activity and liberates antiviral function of the cytidine deaminase APOBEC3G.* FASEB J, 2007. **21**(1): p. 217-22.

31. Neuzil, J., et al., *Classification of mitocans, anti-cancer drugs acting on mitochondria.* Mitochondrion, 2013. **13**(3): p. 199-208.

32. Catapano, M.C., et al., *A simple, cheap but reliable method for evaluation of zinc chelating properties.* Bioorg Chem, 2018. **77**: p. 287-292.

33. Marini, M., et al., *Modulation of caspase-3 activity by zinc ions and by the cell redox state.* Exp Cell Res, 2001. **266**(2): p. 323-32.

34. Wang, L., et al., *Small-Molecule Inhibitors Disrupt let-7 Oligouridylation and Release the Selective Blockade of let-7 Processing by LIN28.* Cell Rep, 2018. **23**(10): p. 3091-3101.

35. Kinumi, T., et al., *Cysteine-106 of DJ-1 is the most sensitive cysteine residue to hydrogen peroxide-mediated oxidation in vivo in human umbilical vein endothelial cells.* Biochem Biophys Res Commun, 2004. **317**(3): p. 722-8.

36. Stramucci, L., A. Pranteda, and G. Bossi, *Insights of Crosstalk between p53 Protein and the MKK3/MKK6/p38 MAPK Signaling Pathway in Cancer.* Cancers (Basel), 2018. **10**(5).

37. Yu, J., et al., *PUMA induces the rapid apoptosis of colorectal cancer cells.* Mol Cell, 2001. **7**(3): p. 673-82.

38. Nakano, K. and K.H. Vousden, *PUMA, a novel proapoptotic gene, is induced by p53.* Mol Cell, 2001. **7**(3): p. 683-94.

Preprints (www.preprints.org) | NOT PEER-REVIEWED | Posted: 6 October 2021 doi:10.20944/preprints202103.0611.v2

39. Doerflinger, M., J.A. Glab, and H. Puthalakath, *BH3-only proteins: a 20-year stock-take.* FEBS J, 2015. **282**(6): p. 1006-16.

40. Edlich, F., *BCL-2 proteins and apoptosis: Recent insights and unknowns.* Biochem Biophys Res Commun, 2018. **500**(1): p. 26-34.

41. Nagata, S., *Apoptotic DNA fragmentation.* Exp Cell Res, 2000. **256**(1): p. 12-8.

Figure legend.

Figure 1. TPEN induces a reduction in the CD34+/CD19+ cell population and activation of CASP-3 in cells from de novo (code number in blue) B-ALL patients.

(A) Representative two-dimensional (2D) density plot showing CD34 (x axis) and CD19 (y axis) flow cytometry performed on leukemic cells (n = 3) from bone marrow (BM) de novo B-ALL patients treated with TPEN (0, 50, 100, 200, and 500 µM) at 37 °C for 24 h; (B) representative histograms showing CASP-3-positive subset from CD34+/CD19+ cells; (C) representative three-dimensional (3D) density plot showing CD34 (x axis), CD19 (z axis), and CASP-3 (y axis) positive cells; (D) and (E) represent the quantitative analysis of the parameters. * $p < 0.05$, ** $p < 0.01$, and *** $p < 0.001$.

Figure 2. TPEN induces a reduction in the CD34+/CD19+ cell population from de novo (code number in blue) and refractory (code number in red) B-ALL patients.

(A) Representative 2D density plot showing CD34 (y axis) and CD19 (x axis) flow cytometry double analyses (Q2) performed on nonleukemic cells (n=3, code 93806, 51893, 86340), and on leukemic cells (de novo (n = 5) and refractory (n = 6) B-ALL) untreated or treated with

Preprints (www.preprints.org) | NOT PEER-REVIEWED | Posted: 6 October 2021 doi:10.20944/preprints202103.0611.v2

TPEN (100 µM) at 37 °C for 24 h; (B) represents the quantitative analysis of the data from quadrant Q2. * $p < 0.05$, ** $p < 0.01$, and *** $p < 0.001$.

Figure 3. TPEN induces the activation of CASP-3 in the CD34+/CD19+ cell population from de novo (code number in blue) and refractory (code number in red) B-ALL patients.

(A) Representative 3D density plot showing the flow cytometry analysis of CD34 (x axis), CD19 (z axis), and CASP-3 (y axis) positive cells performed on nonleukemic cells (n=3, code 93806, 51893, 86340), and on leukemic cells (de novo (n = 5) and refractory (n = 6) B-ALL) untreated or treated with TPEN (100 µM) at 37 °C for 24 h; (B) represents the quantitative analysis of the data. * $p < 0.05$, ** $p < 0.01$, and *** $p < 0.001$.

Figure 4. TPEN induces simultaneous activation of CASP-3 and oxidation of DJ-1 in cells from de novo and refractory B-ALL patients.

(A) Representative 2D density plot showing CASP-3 (y axis) and ox-DJ-1 (x axis) flow cytometry double analyses (Q2) performed on nonleukemic cells (n=3, code 93806, 51893, 86340), and on leukemic cells (de novo and refractory B-ALL) untreated or treated with TPEN (100 µM) at 37 °C for 24 h; (B) represents the quantitative analysis of the data from quadrant Q2. * $p < 0.05$, ** $p < 0.01$, and *** $p < 0.001$.

Preprints (www.preprints.org) | NOT PEER-REVIEWED | Posted: 6 October 2021 doi:10.20944/preprints202103.0611.v2

Figure 5. TPEN induces the activation of PUMA in cells from de novo and refractory B-ALL patients

(A) Representative 3D density plot showing the flow cytometry analysis of CD34 (x axis), CD19 (z axis), and PUMA (y axis) positive cells performed on nonleukemic cells (n=3, code 93806, 51893, 86340), and on leukemic cells (de novo and refractory B-ALL, n=8) un-treated or treated with TPEN (100 µM); (B) represents the quantitative analysis of the data. * $p < 0.05$, ** $p < 0.01$, and *** $p < 0.001$.

Figure 6. TPEN induces activation of TP53 and PUMA in cells from de novo and refractory B-ALL patients.

(A) Representative 2D density plot showing PUMA (y axis) and TP53 (x axis) flow cytometry double analyses (Q2) performed on nonleukemic cells (n=3, code 93806, 51893, 86340), and on leukemic cells (de novo and refractory B-ALL, n=8) untreated or treated with TPEN (100 µM) at 37 °C for 24 h; (B) represents the quantitative analysis of the data from the Q2 quadrant. * $p < 0.05$, ** $p < 0.01$, and *** $p < 0.001$.

Preprints (www.preprints.org) | NOT PEER-REVIEWED | Posted: 6 October 2021 doi:10.20944/preprints202103.0611.v2

Legend Table

Table 1. Characteristic profile of blood and bone marrow (BM) from patients without leukemia (code number in black), with de novo (code number in blue) and refractory (code number in red) B-cell acute lymphoblastic leukemia (B-ALL) pediatric patients untreated (UNT) or treated with TPEN.

Intra-group and inter-group statistical comparison were performed according to Student-t analysis. * $p < 0.05$, ** $p < 0.01$, and *** $p < 0.001$.

Abbreviations: NA, not apply; NP, not performed; UNT, untreated; WBC, white blood count; X= mean; S.D. standard deviation

Code	WBC	Blasts (%)	Sex	Age (years)	Karyotype	Immunophenotype	CD34+/CD19+ /CASP3+ UNT (%)	CD34+/CD19+ /CASP3+ 100 µM TPEN (%)
51863	NP	0.6%	M	16	NP	NP	3	2
93806	NP	0.4%	F	8	NP	NP	2	5
86340	NP	0.5%	M	12	NP	NP	1	2
X±S.D.				**12 ± 4.0**			**2.0 ± 1.0**	**3.0 ± 1.7**
72750	139,300	85%	M	13	Complex karyotype	**97% B cells:** CD45w, CD19+, CD79a+, CD22+, CD20+/-, CD24+, CD9+, CD10+, CD34+/-, CD38+, TdT+,	5	40

Preprints (www.preprints.org) | NOT PEER-REVIEWED | Posted: 6 October 2021 doi:10.20944/preprints202103.0611.v2

						CD123w, CD66+/-, cIgM+. cMPO-, CD13-, CD33-, CD117-, cCD3-, sIgM-		
19105	10,500	50%	F	12	Complex karyotype	**95% B cells:** CD45w/-, CD34 +/-, CD19+, CD79a+, CD20+/-, CD10+, CD38+, Tdt+, CD22+, CD24+, CD95+	3	22
62232	81,300	92%	M	8	Complex karyotype	**92% B cells:** CD45w, CD19+, CD79a+, CD22+, TdT+, CD10+, CD20+/-, CD24+, CD9+	5	28
11630	27,900	85%	F	7	46, XX, del(6)(q21)[6]/46, XX[15]	**89% B cells:** CD45w, CD19+, CD79a+, CD34+, CD22+, TdT+, CD20 het, CD10+, CD38+, CD123+, CD13 partial, CD33 partial, CD24+. cIgU-, sIgM-, MPO-, CD7-, CD3-, CD66c-, CD21-NG2-, CD15-.	5	29
04168	19,000	75%	F	2.5	54–58, XX, +X, +X, +6, +10, +14, +15, +17,	**87% B cells:** CD45w, CD34+, CD79a+, CD19+, CD20 het, CD10+, CD38+,	3	34

Preprints (www.preprints.org) | NOT PEER-REVIEWED | Posted: 6 October 2021 doi:10.20944/preprints202103.0611.v2

					+18, +21, +21, +21[17]/46, XX[2]	TdT+, CD22+, CD66c+, CD123+, CD13+, CD9+, CD24+. cIgU-, sIgM-, MPO-, CD7-, CD3-, CD33-, NG2-		
X±S.D.				**8.5 ± 3.8**			**4.2 ± 1.0**	**30.6 ± 6.0*** **
32765	166,620	90%	F	13	t(9:22)-, MLL+	**97% B cells:** CD45w, CD19+, CD79A+, CD22+, TdT het, CD34 het, CD38+, CD15+, NG2CD24 het, CD9+ y CD123+. CD3-, CD7-, MPO-, CD10-, cIgU-, sIgM-, CD66C-, CD21-, CD13-, CD33-, CD20-. CD15 and NG2 + associated to 11q2.3.	3	35
48983	23,300	50%	F	9	Complex Karyotype hyperdiploid mosaicism, T12:21+	**84% B cells:** CD45w, CD34+, CD19+, CD79a+, CD22+, CD10+, CD20 het, TdT+, CD9+, CD24+, CD123+, CD66c+. Neg. for CD3, MPO, CD7, CD13, CD33, IgM, cIgU, CD21.	3	35

Preprints (www.preprints.org) | NOT PEER-REVIEWED | Posted: 6 October 2021 doi:10.20944/preprints202103.0611.v2

06600	2540	61%	M	16	NP	**61% B cells:** CD45w, CD34+, CD19+, CD20 het, CD10+, CD38+, CD66c+ y CD123+. CD15-, NG2-, CD21-	6	12
79426	4700	16%	F	5	51–54, XX, +del(6)(q23), +8, +14, +14, +21, +22[cp7]/46, XX[20]	**84% B cells:** CD19+, CD34 het., CD10+, CD38+, CD66c+, CD123+. CD45-, CD20-, CD15-, NG2-	4	24
81571	3500	12%	M	3.5	44–45, XY, dic(1;12)(q21;p13), t(5;17)(q35;q21), der(7;12)(q10;10), i(12)(p10)[cp5]/46, XY[5]	**96%B cells:** CD19+, CD34 partial, CD10+, CD38+, CD66c+, CD123 partial, CD15 partial CD45-, CD20-, NG2-	5	35
20978	5,400	86%	F	4	NP	**77% B cells:** CD45w, CD19+, CD34+, CD20 het, CD10+, CD38+, CD66c partial	3	50
X±S.D.				**8.4 ± 4.7**			**4.0 ± 1.1**	**31.8 ± 11.6*** **

Preprints (www.preprints.org) | NOT PEER-REVIEWED | Posted: 6 October 2021 doi:10.20944/preprints202103.0611.v2

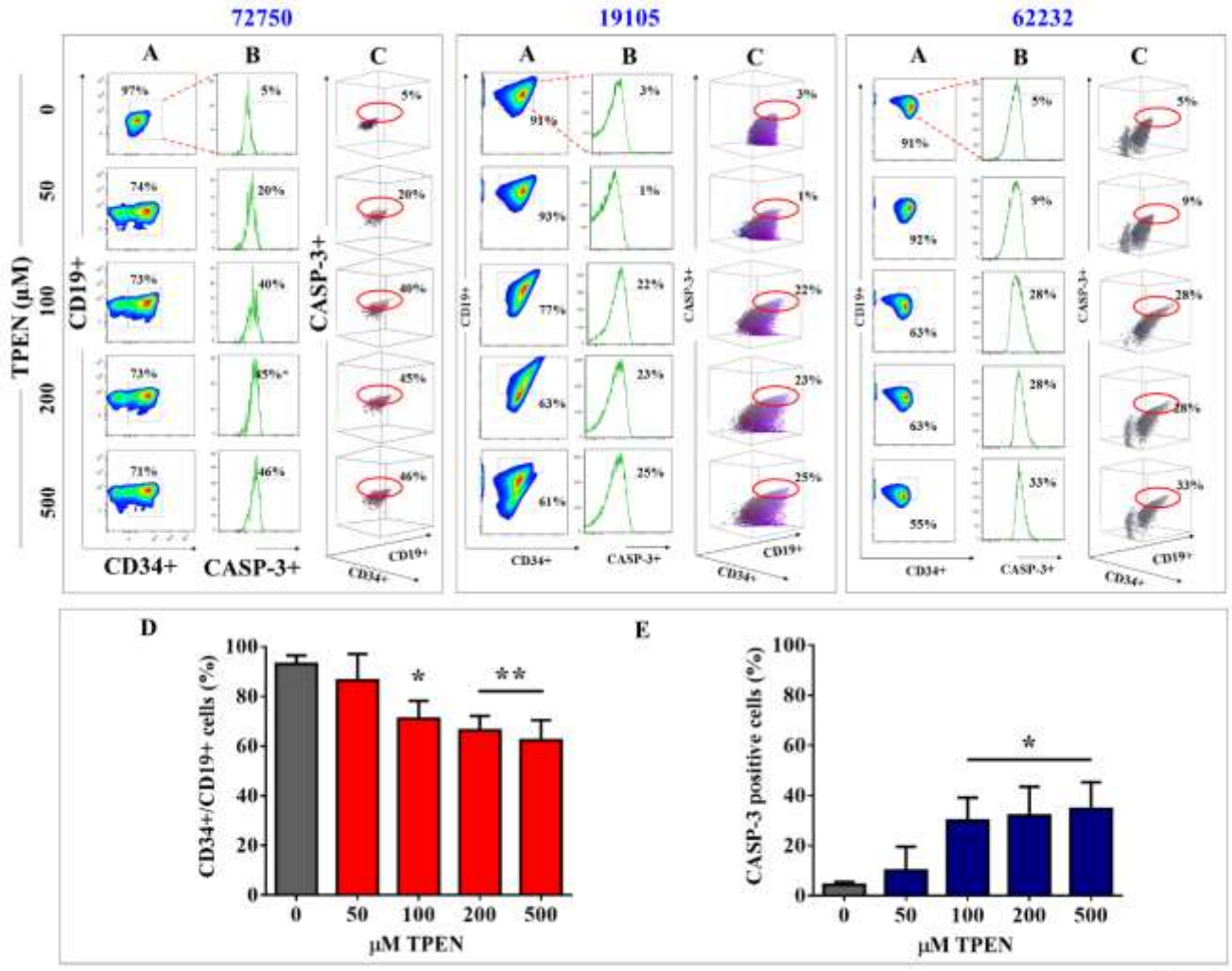

Figure 1

Preprints (www.preprints.org) | NOT PEER-REVIEWED | Posted: 6 October 2021 doi:10.20944/preprints202103.0611.v2

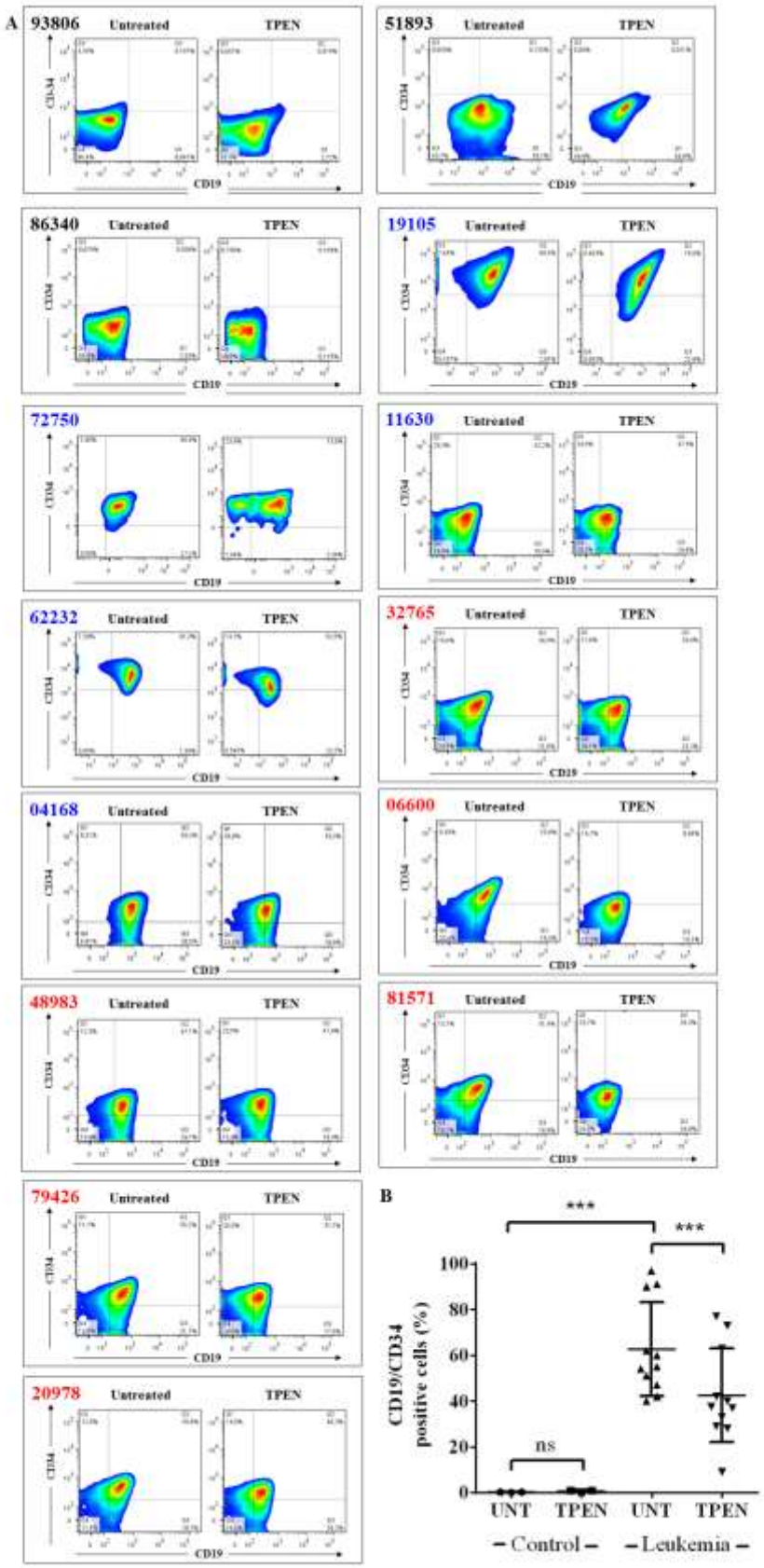

Figure 2

Preprints (www.preprints.org) | NOT PEER-REVIEWED | Posted: 6 October 2021 doi:10.20944/preprints202103.0611.v2

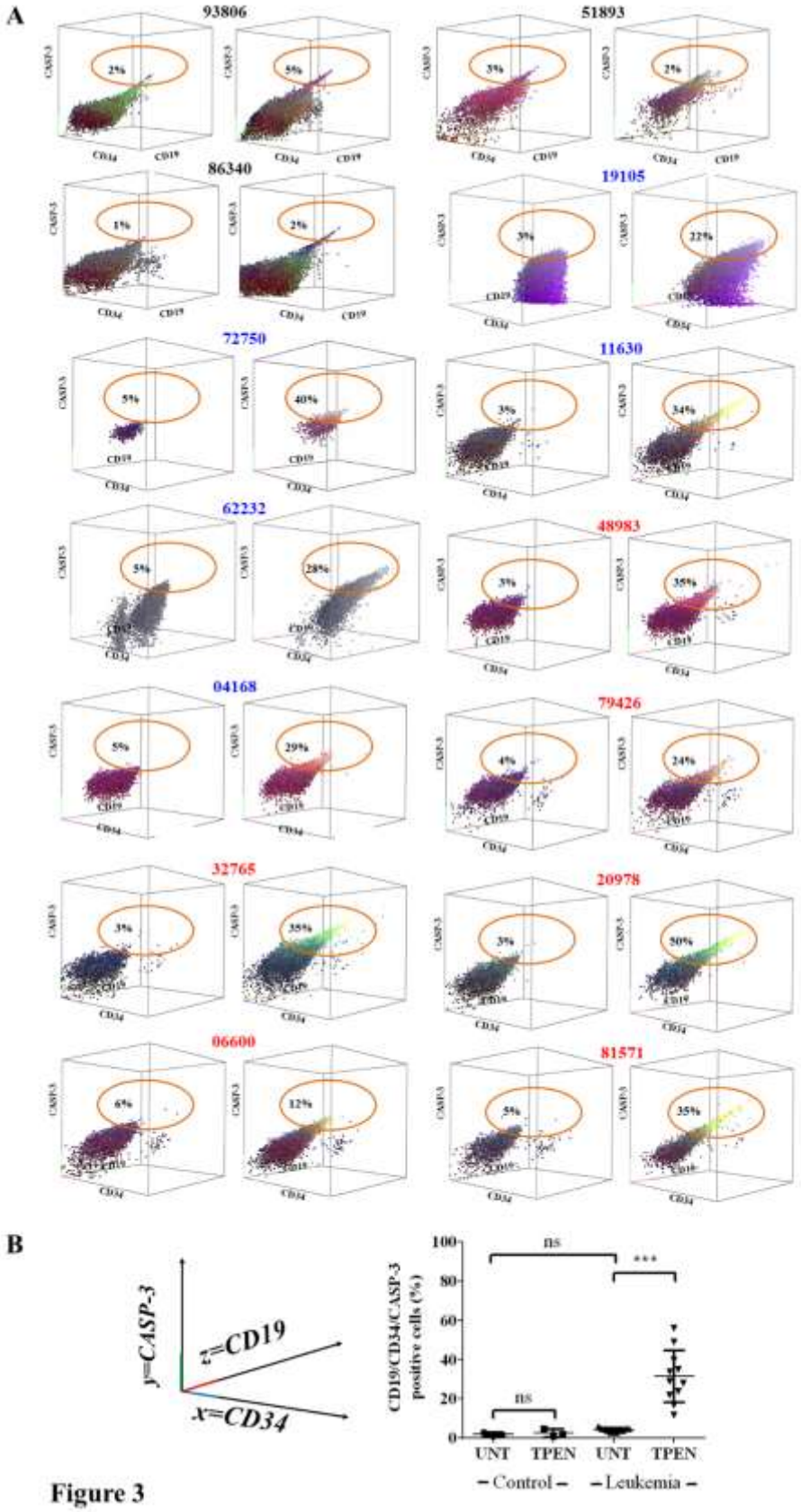

Figure 3

Preprints (www.preprints.org) | NOT PEER-REVIEWED | Posted: 6 October 2021 doi:10.20944/preprints202103.0611.v2

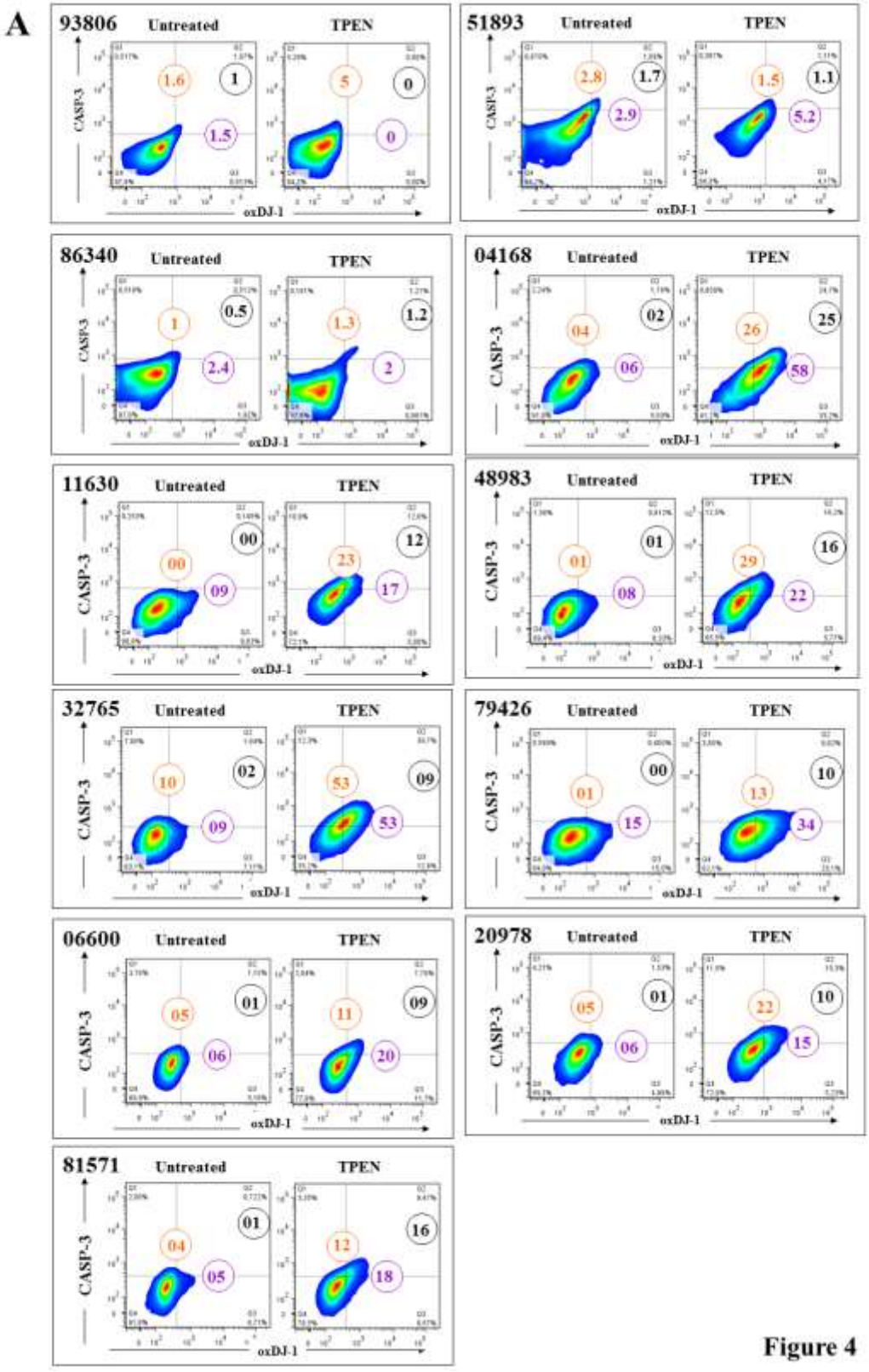

Figure 4

Preprints (www.preprints.org) | NOT PEER-REVIEWED | Posted: 6 October 2021 doi:10.20944/preprints202103.0611.v2

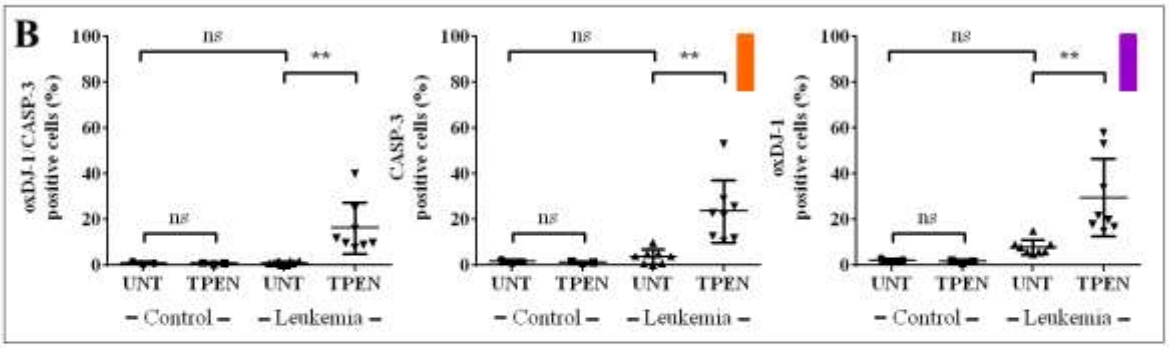

Figure 4

Preprints (www.preprints.org) | NOT PEER-REVIEWED | Posted: 6 October 2021 doi:10.20944/preprints202103.0611.v2

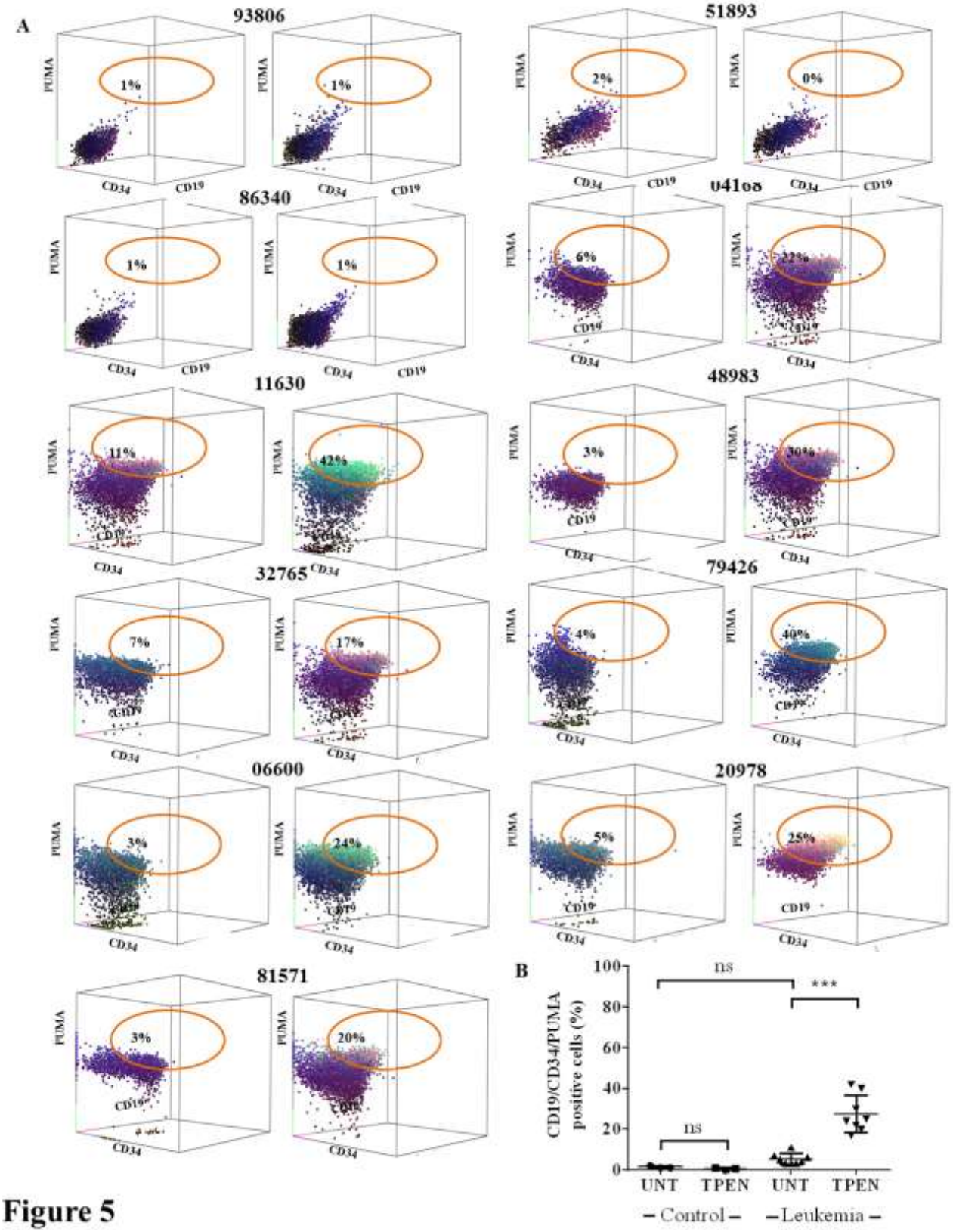

Figure 5

Preprints (www.preprints.org) | NOT PEER-REVIEWED | Posted: 6 October 2021 doi:10.20944/preprints202103.0611.v2

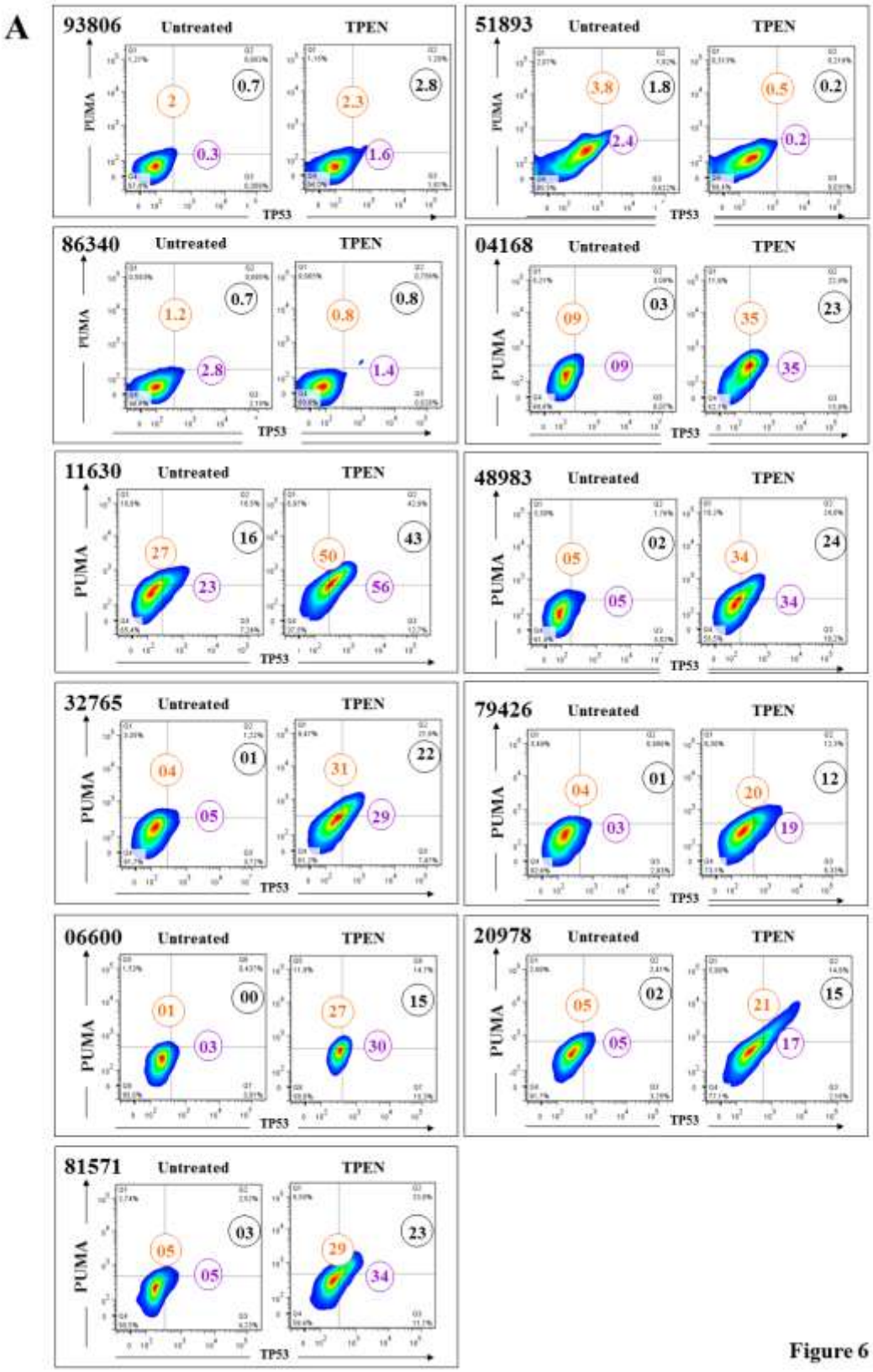

Figure 6

Preprints (www.preprints.org) | NOT PEER-REVIEWED | Posted: 6 October 2021 doi:10.20944/preprints202103.0611.v2

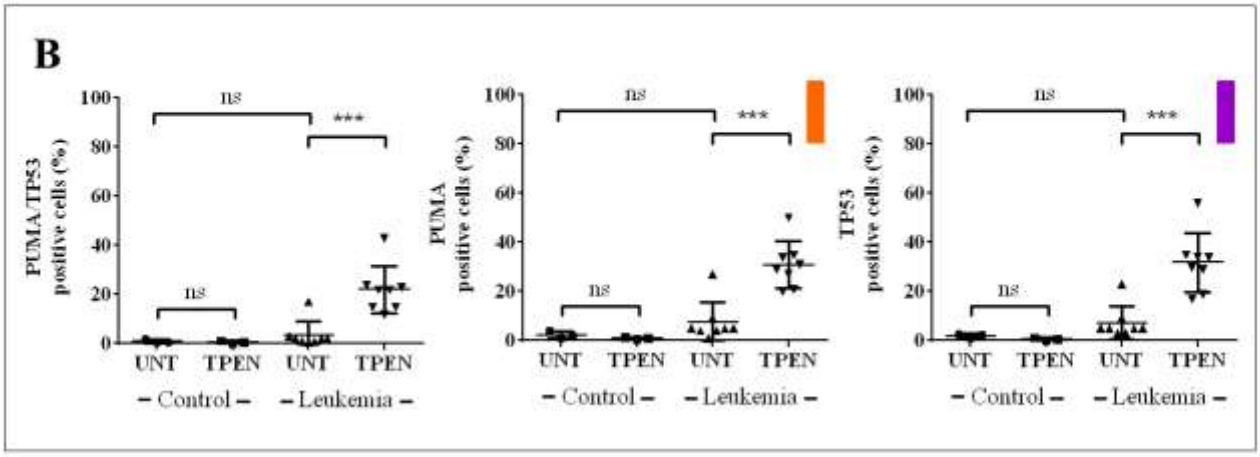

Figure 6